

# Overexpression of Manganese Superoxide Dismutase Suppresses Tumor Formation by Modulation of Activator Protein-1 Signaling in a Multistage Skin Carcinogenesis Model<sup>1</sup>

Yunfeng Zhao, Yi Xue, Terry D. Oberley, Kelley K. Kinningham, Shu-Mei Lin, Hsiu-Chuan Yen,<sup>2</sup> Hideyuki Majima,<sup>3</sup> Judy Hines, and Daret St. Clair<sup>4</sup>

Graduate Center for Toxicology, University of Kentucky, Lexington, Kentucky 40536 [Y. Z., K. K. K., S-M. L., H-C. Y., H. M., J. H., D. S. C.], and Department of Pathology [Y. X., T. D. O.] and Veterans Affairs Hospital [T. D. O.], University of Wisconsin, Madison, Wisconsin 53705

## ABSTRACT

Manganese superoxide dismutase (MnSOD) is a nuclear encoded primary antioxidant enzyme localized in mitochondria. Because expression of MnSOD plays a major role in maintaining cellular redox status and reactive oxygen species are known to play a role in signal transduction and carcinogenesis, we investigated the role of MnSOD in the development of cancer using a two-stage [7,12-dimethylbenz(*a*)-anthracene plus 12-*O*-tetradecanoylphorbol-13-acetate (TPA)] skin carcinogenesis model. Female transgenic mice expressing the human *MnSOD* gene in the skin and their nontransgenic counterparts were used in this study. Pathological examination demonstrated significant reduction of papilloma formation in transgenic mice. Quantitative analysis of 4-hydroxy-2-nonenal-modified proteins showed greater accumulation of oxidative damage products in nontransgenic compared with transgenic mice, and this oxidative damage was demonstrated to be present in both mitochondria and nucleus. TPA increased activator protein-1 (AP-1) binding activity within 6 h in nontransgenic mice, but increased AP-1 binding activity was delayed in the transgenic mice. Electrophoretic mobility shift assay, transcription of the target genes, and Western analysis studies indicated that the increased AP-1 binding activity was attributable to induction of the Jun but not the Fos protein families. Overexpression of MnSOD selectively inhibited the TPA-induced activation of protein kinase C $\epsilon$  and prevented subsequent activation of c-Jun NH<sub>2</sub>-terminal kinase in response to TPA. Overall, these results indicate that MnSOD regulates both cellular redox status and selectively modulates PKC $\epsilon$  signaling, thereby delaying AP-1 activation and inhibiting tumor promotion, resulting in reduction of tumors in MnSOD transgenic mice.

## INTRODUCTION

MnSOD<sup>5</sup> is one of the major cellular defense enzymes that protects against toxic effects of ROS. Recent evidence suggested the possibility that MnSOD may function as a new type of tumor suppressor gene. Previous investigations from this and other laboratories have demonstrated that tumor cells have abnormal MnSOD activity (1–3), and overexpression of MnSOD reduced tumorigenicity and metastatic capability of many tumor types (4–6). However, despite the positive correlation between increased expression of MnSOD and the suppression of cancer, the specific stage and mechanisms by which MnSOD acts to suppress cancer development is unknown.

The multistage skin carcinogenesis model in mice involves three

well-defined stages: initiation, promotion, and progression. This model has been used to evaluate carcinogens, investigate chemicals that exhibit antitumor promotion activity, and determine biochemical and molecular events accruing in each stage (7). It has been established that polycyclic aromatic hydrocarbons, such as DMBA, can act either as a complete carcinogen or as an initiator of mouse skin carcinogenesis. A large dose of DMBA, acting as a complete carcinogen, is capable of inducing skin tumors in mice; in this model, papillomas appear after a short latency period (8). In contrast, application of a subthreshold dose of DMBA, followed by repetitive treatments with a tumor promoter such as the phorbol ester TPA, will also induce tumors. In the latter protocol, initiation is achieved by mutational activation of the *Ha-ras* proto-oncogene (7, 9). Mutation in the *Ha-ras* gene is thought to result in a population of initiated cells that remain dormant until stimulated to expand clonally upon treatment with promoters, resulting in the formation of papillomas (7).

As one of the most thoroughly studied classes of tumor promoters, phorbol esters are known to act by mediating signal transduction to the nucleus through activation of kinases and inactivation of phosphatases, respectively (7, 10). Treatment with TPA also produces ROS, with resultant oxidative damage to macromolecules, leading to changes in cellular redox status (11, 12). It is now well recognized that superoxide radicals, a major intracellular ROS, are not just a toxic by-product of molecular oxygen but are also signaling molecules. Thus, superoxide radicals can transmit important information to the cellular genetic machinery (13). We have shown previously that overexpression of MnSOD modulates the activity of the Jun-associated transcription factors in cancer cells *in vitro*. However, whether MnSOD will modulate these transcription factors in intact animals is unknown. Furthermore, the upstream signaling events leading to the MnSOD-modulated activation of these transcription factors remain to be investigated.

In this study, we have developed a line of transgenic mice expressing the human *MnSOD* gene in the skin. We have investigated the extent to which MnSOD suppresses cancer development, quantitated the formation of oxidative damage products, measured the activity and expression of oncoproteins and their target genes, and analyzed the upstream signaling pathways using transgenic mice and their nontransgenic littermates. Our results demonstrate that MnSOD overexpression modulates each of these critical events *in vivo*.

Received 4/3/01; accepted 6/12/01.

The costs of publication of this article were defrayed in part by the payment of page charges. This article must therefore be hereby marked *advertisement* in accordance with 18 U.S.C. Section 1734 solely to indicate this fact.

<sup>1</sup> This work was supported by NIH Grants CA 73599 and CA 73599-S1.

<sup>2</sup> Present address: Chang Gung University, Tao-Yuan 333, Taiwan, Republic of China.

<sup>3</sup> Present address: National Institute of Radiological Sciences, Chiba 263-8555 Japan.

<sup>4</sup> To whom requests for reprints should be addressed, at Graduate Center for Toxicology, University of Kentucky, Lexington, KY 40536. Phone: (859) 257-3956; Fax: (859) 323-1059; E-mail: dstcl00@pop.uky.edu.

<sup>5</sup> The abbreviations used are: MnSOD, manganese superoxide dismutase; ROS, reactive oxygen species; DMBA, 7,12-dimethylbenz(*a*)-anthracene; TPA, 12-*O*-tetradecanoylphorbol-13-acetate; PMSF, phenylmethylsulfonyl fluoride; 4-HNE, 4-hydroxy-2-nonenal; TBS, Tris-buffered saline; EMSA, electrophoresis mobility shift assay; AP-1, activator protein-1; JNK, c-Jun NH<sub>2</sub>-terminal kinase; PKC, protein kinase C.

## MATERIALS AND METHODS

### Mice Strain

Human MnSOD transgenic mice were generated in our laboratory as described previously (14). Briefly, human MnSOD cDNA was introduced into pronuclei of fertilized eggs by microinjection. Mice used for producing transgenic mice were the F<sub>1</sub> progeny of C57BL/6 mice crossed with C3H hybrid (B6C3) mice that were purchased from Harlan Sprague Dawley (Indianapolis, IN). The identification of MnSOD transgenic mice has been reported previously (14). For the skin carcinogenesis experiments, female transgenic mice

that exhibited a high level of MnSOD activity (TgH) and their female non-transgenic littermates (nTg) were used.

### Expression of the Human *MnSOD* Gene in the Skin of Transgenic Mice

**Northern Analysis.** Total RNA from dissected skin tissues of transgenic and nontransgenic mice was isolated by the guanidine isothiocyanate method (15). Thirty  $\mu\text{g}$  of total RNA were separated by formaldehyde-agarose (1.1%) gel electrophoresis and transferred to a Nytran membrane (Schleicher & Schuell, Keene, NH). The membrane was air dried, baked, prehybridized, and hybridized with  $^{32}\text{P}$ -labeled MnSOD cDNA probe and subsequently washed under high stringency conditions as described previously (16). The membrane was exposed to a Kodak XAR film at  $-80^\circ\text{C}$ . The level of  $\beta$ -actin RNA was used as an internal loading control.

**Western Analysis of the Human *MnSOD* Gene Product.** Thirty  $\mu\text{g}$  of tissue homogenate were separated on a 10% SDS-PAGE gel according to the method of Landriscina (17). To detect levels of human MnSOD protein in the skin, rabbit antihuman MnSOD antibody (kindly provided by Dr. Larry Oberley at the University of Iowa, Iowa City, IA) was used.

**Immunogold Electron Microscopy.** The localization of the human MnSOD protein in mitochondria was accessed by electron microscopy as described previously (14).

**SOD Activity Gel.** SOD activity gel was performed following our method published previously (6). Protein concentration was measured by a colorimetric assay (Bio-Rad Laboratories, Richmond, CA).

### Two-Stage Carcinogenesis

Hair from the back of female mice, 6–8 weeks of age, were shaved 2 days prior to application of vehicle or carcinogen. Mice in the resting stage of hair cycle were chosen for subsequent treatment. A single dose of 20 nmol of DMBA (Sigma Chemical Co., St. Louis, MO) dissolved in DMSO was painted on each mouse. After 2 weeks, 4  $\mu\text{g}$  of TPA, also dissolved in DMSO, was applied daily to the same area 5 days/week for 14 weeks. After euthanasia, skin from each mouse was removed and fixed in 4% neutral buffer formaldehyde for subsequent pathological examination. For study of the early events of carcinogenesis by biochemical and molecular analyses, TPA was applied for no more than 1 week after DMBA initiation.

### Light Microscopy

Skin tissues were fixed in 4% formaldehyde in PBS for 1 h. After rinsing with PBS, tissues were dehydrated with graded ethanol and embedded in paraffin. Paraffin sections were cut at 4  $\mu\text{m}$  and mounted on glass slides. Tissue sections were stained with H&E, and H&E sections were analyzed in a blinded fashion by a pathologist (T. D. O.) to determine the number of papillomas.

### Immunogold Labeling of 4-HNE-modified Proteins

LR white embedded tissue blocks were trimmed and sectioned. Thin sections were mounted on 1% collodion membrane-coated nickel grids. Sections were rinsed and blocked with BSA-C block solution for 30 min to block nonspecific staining and then incubated with primary antibody at  $4^\circ\text{C}$  overnight. Rabbit anti-4-HNE polyclonal antibody (kindly provided by Dr. Luke Szveda, Case Western Reserve University, Cleveland, OH) was used at a dilution of 1:60. After incubation with primary antibody overnight at  $4^\circ\text{C}$ , grids were rinsed in four changes of TBS washing buffer for 5 min each and one change of alkaline TBS for 10 min. Then the grids were incubated with diluted (1:75) gold conjugated secondary antibody (gold-conjugated goat anti-rabbit IgH+L; GAR15 BB International) for 90 min at room temperature. The sections were washed in two changes of TBS wash buffer for 10 min, each followed by two changes of distilled water; the grids were counterstained with 7.5% uranyl acetate, observed, and photographed with a Hitachi H-600 transmission electron microscope. All of the sections for quantitative Immunogold electron microscopy analysis were stained simultaneously under the same conditions.

### Quantitative Analysis of Oxidative Damage Products

Micrographs were randomly taken at  $\times 10,000$  from whole epidermis (in areas where the epidermis was thin) or from selected equal numbers of

keratinocytes (identified by the presence of desmosomes, keratohyaline granules, and tonofilaments) from stratum germinativum, spinosum, and basal cells of the epidermis (for areas of the skin which were thick). Non-keratinocytes, stratum corneum, and the cells of the hair follicles were not included in the analysis. The area of mitochondria, cytoplasm, and nucleus in selected epidermal cells and the densities of Immunogold labeling of 4-HNE-modified protein were quantitatively analyzed with image analysis software-Scion Image  $\beta$  4.02 (Scion Corp., Frederick, MD) with a PC computer (Dell OptiPlex GX200). The mean values were obtained from an average of 30 cells from each group. Statistical analysis was performed by Student's *t* test. Results were presented as the means  $\pm$  SD.

### Preparation of Nuclear Extract from Skin Samples

Skin cells were stripped off using an autoclaved glass slide and suspended in 400  $\mu\text{l}$  of buffer A [10 mM HEPES-KOH with 1.5 mM  $\text{MgCl}_2$ , 10 mM KCl, 0.2 mM PMSF, 5  $\mu\text{M}$  of DTT, and protease inhibitors (5  $\mu\text{g}/\text{ml}$  of pepstatin, leupeptin and aprotinin)]. After gently vortexing and centrifugation, the supernatant was transferred to a new tube. The pellet was resuspended in 400  $\mu\text{l}$  buffer A, and homogenized by a 10-ml Wheaton homogenizer (15 times up-and-down). The supernatant was kept on ice for 30 min, and then 25  $\mu\text{l}$  of 10% NP-40 were added and vortexed vigorously for 25 s. Lysate was centrifuged at 14,000 rpm (or  $17,500 \times g$ ) for 1 min. The supernatant was collected and subsequently referred to as cytoplasmic fraction. The pellet was dissolved in 120  $\mu\text{l}$  of buffer B [20 mM HEPES-KOH with 1.5 mM  $\text{MgCl}_2$ , 420 mM NaCl, 35% glycerol, 0.2 mM PMSF, 5  $\mu\text{M}$  of DTT, and 0.2 mM EDTA (pH 8.0)] containing the protease inhibitors (5  $\mu\text{g}/\text{ml}$  of pepstatin, leupeptin, and aprotinin). The sample was kept on ice for 30 min and centrifuged at 12,000 rpm for 5 min, and the supernatant was identified as nuclear extract and was frozen at  $-80^\circ\text{C}$ . Protein concentration was measured by a colorimetric assay (Bio-Rad Laboratories, Richmond, CA).

### Preparation of Total Cell Lysate, Cytosol, and Membrane Fractions

Skin cells were stripped and extracted by homogenization as described above except 1 ml of homogenization buffer [20 mM HEPES (pH 7.0), 5 mM EGTA, 10 mM 2-mercaptoethanol, 1 mM PMSF, 1  $\mu\text{g}/\text{ml}$  leupeptin, 1  $\mu\text{g}/\text{ml}$  aprotinin, and 1  $\mu\text{g}/\text{ml}$  pepstatin] was used instead of buffer A. The total cell lysate, cytosol, and membrane fraction were prepared as described previously (18). Briefly, after homogenization, the lysate was centrifuged ( $50 \times g$  or 600 rpm for 5 min) to remove tissue debris, the resulting supernatant was designated total cell lysate, and 100  $\mu\text{l}$  of it was kept at  $-80^\circ\text{C}$ . The remainder of the total cell lysate was centrifuged at  $10,000 \times g$  for 1 h at  $4^\circ\text{C}$ ; the supernatant was designated as cytosolic fraction and kept at  $-80^\circ\text{C}$ . The  $10,000 \times g$  pellet was washed with homogenization buffer once and then suspended in 140  $\mu\text{l}$  of the homogenization buffer containing 0.5% Triton X-100 and incubated on ice for 30 min with intermittent vigorous vortexing. After centrifuging ( $14,000 \times g$ , 30 min), the resulting supernatant was designated as membrane fraction and stored at  $-80^\circ\text{C}$ .

### EMSAs

AP-1-DNA binding activity was analyzed in nuclear extracts. The AP-1 double-strand oligonucleotide (5'-CGCTTGATGAGTCAGCCGAA-3') was purchased from Promega Corp. (Madison, WI). A 25- $\mu\text{l}$  reaction solution contained 6  $\mu\text{g}$  of nuclear extract, 5  $\mu\text{l}$  of  $5\times$  binding buffer [50 mM Tris-HCl (pH 7.4), with 20% glycerol, 5 mM  $\text{MgCl}_2$ , 2.5 mM EDTA, 5 mM DTT, and 0.25 mg/ml poly(deoxyinosinic-deoxycytidylic acid)] and 50,000 cpm labeled probe. After 20 min of incubation at room temperature, 3  $\mu\text{l}$  of  $10\times$  loading buffer were added, and samples were separated on a 6% native polyacrylamide gel for 3–4 h. DNA-protein complexes were visualized by exposing the gels to Kodak film at  $-80^\circ\text{C}$ . For supershift assays, the nuclear extract was preincubated with 5  $\mu\text{g}$  of respective antibody to each member of the AP-1 family (anti-c-Jun, Jun B, Jun D, c-Fos, and Fra-1, all from Santa Cruz Biotechnology, Santa Cruz, CA) for 1 h at room temperature, and then the same steps as described above were followed.

### Western Blot Analysis

Ten  $\mu\text{g}$  of the membrane fraction were separated on a 10% SDS-PAGE gel to detect the levels of PKC. Ponceau staining was used to assess transfer of

protein onto the nitrocellulose membrane. The membrane was washed with distilled water to remove excess stain and blocked in Blotto [5% milk, 10 mM Tris-HCl (pH 8.0), 150 mM NaCl, and 0.05% Tween 20] for 2 h at room temperature. Membranes were probed with specific rabbit polyclonal antibodies against each PKC isoform (PKC $\alpha$ ,  $\beta$ I,  $\beta$ II,  $\delta$ ,  $\epsilon$ ,  $\lambda$ ,  $\mu$ , and  $\zeta$ , all from Santa Cruz Biotechnology) at a 1:1000 dilution. To detect the phosphorylated form of JNK (pJNK), the cytosolic fraction was loaded, and anti-pJNK antibody (G-7, sc-6254; Santa Cruz Biotechnology) was used at 1:1000 dilution. To detect Jun D and c-Jun, 30  $\mu$ g of the nuclear extract were loaded on a 10% SDS-PAGE gel. After transferring and blocking, a rabbit polyclonal antibody against Jun D was used (Santa Cruz Biotechnology) at a 1:1000 dilution. After visualization of protein bands, the membrane was stripped and reprobed with an anti-c-Jun antibody (Santa Cruz Biotechnology) at a 1:1000 dilution. Before adding the secondary antibody, the membrane was washed twice with TBST (10 mM Tris-HCl with 150 mM NaCl and 0.05% Tween 20), and then the membrane was incubated with horseradish peroxidase-conjugated secondary antibodies (Santa Cruz Biotechnology) at a 1:4000 dilution. The final washing steps included three times (5 min each) with TBST and two times (5 min each) with TBS (10 mM Tris-HCl with 150 mM NaCl). The antibody bands were visualized by the enhanced chemiluminescence detection system (ECL; Amersham Pharmacia Biotech, Piscataway, NJ).

## RESULTS

**Expression and Localization of the Human *MnSOD* Gene in the Skin of TgH Mice.** To verify that the human *MnSOD* gene in the transgenic mice was expressed and properly translated into active protein, the presence of the human *MnSOD* mRNA and protein in mouse skin was assessed, and *MnSOD* activity was measured. mRNA levels of the human *MnSOD* gene were determined by Northern analysis. Fig. 1A is a representative blot demonstrating that in the nTg mouse, human *MnSOD* mRNA was not detectable, whereas the 1-kb mRNA band corresponding to the human *MnSOD* cDNA was present in the transgenic mouse.

Western blot shows that the level of *MnSOD* protein was also increased in the skin of transgenic mouse (Fig. 1B). The enzymatic function of the human *MnSOD* was confirmed by SOD activity gel (Fig. 1C). In the skin, the *MnSOD* activity in the nTg and TgH was determined to be  $83 \pm 19$  and  $171 \pm 32$  units/mg, respectively. Immunogold analysis indicated higher levels of *MnSOD* in the TgH mice (data not shown) and showed that the human *MnSOD* was localized in the mitochondria (Fig. 1D). These results demonstrate that authentic human *MnSOD* was expressed and properly targeted to the mitochondria.

**Tumor Formation.** Tumor types and incidence were determined by pathological examination of H&E sections. The data in Table 1 show that there were no papillomas identified in the transgenic and nontransgenic mice treated with vehicle alone. Seventy-eight % of the nTg mice developed papillomas, whereas 50% of the TgH mice developed papillomas. There were 19 papillomas in the nTg mice, averaging 2.1 papillomas/mouse, compared with 9 papillomas in the TgH mice, averaging 0.75 papillomas/mouse. No carcinomas were identified in any of the mice. The results indicate that overexpression of *MnSOD* reduced tumorigenicity in this two-stage carcinogenesis model.

**Oxidative-Damage Products.** It has been demonstrated previously by other laboratories that oxidative stress is present in DMBA/TPA-induced carcinogenesis (19, 20). We determined the levels of protein adducts of a highly toxic aldehyde product of lipid peroxidation, 4-HNE, in mouse skin. 4-HNE-modified protein levels were increased 6 h after TPA treatment in both the nTg mice and TgH mice, and the increase was greater in the nTg mice ( $\sim$ 3-fold) than the TgH mice ( $\sim$ 2-fold), as shown in Table 2. The increase of 4-HNE-modified proteins occurred to a significant extent in both nucleus and mitochondria but much less in cytoplasm. The levels of 4-HNE-

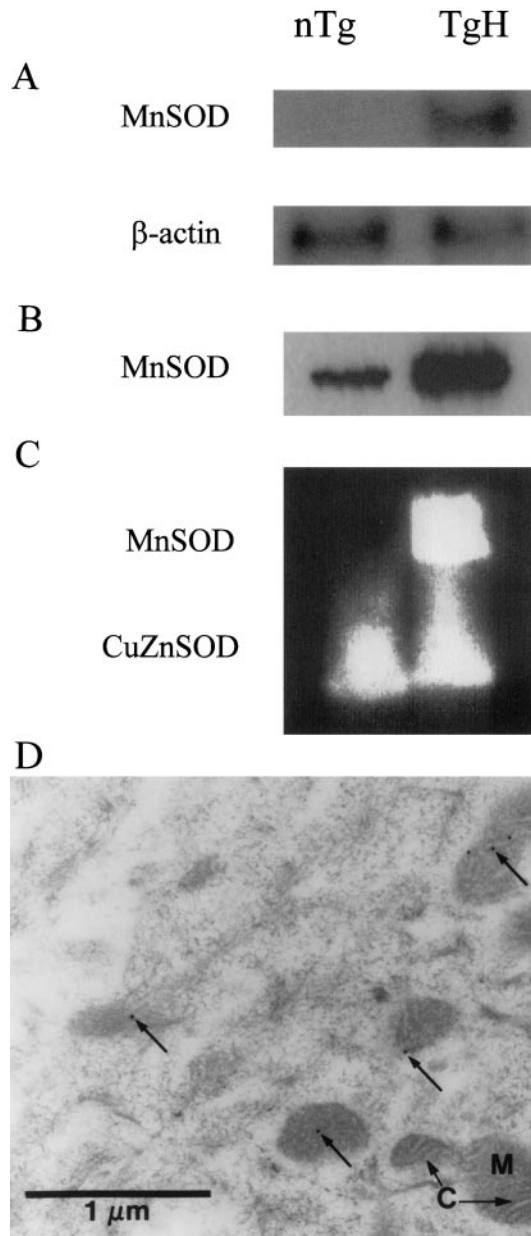


Fig. 1. Expression of human *MnSOD* in mouse skin. A, Northern analysis of human *MnSOD* RNA. Thirty  $\mu$ g of total RNA from each sample were electrophoresed and transferred. Blot was hybridized with  $^{32}$ P-labeled human *MnSOD* cDNA or  $\beta$ -actin probe. B, Western analysis of human *MnSOD* protein levels in the skin. Thirty  $\mu$ g of tissue homogenate were separated on a 10% SDS-PAGE gel, electrotransferred to a nitrocellulose membrane, and detected with polyclonal antibody against human *MnSOD*. C, SOD activity gel. Two hundred  $\mu$ g of protein were separated on a native polyacrylamide gel and stained for SOD activity by photo-induced nitro blue tetrazolium reduction. D, Immunogold localization of *MnSOD* in mitochondria. LR white embedded sections were stained with antibody against human *MnSOD*. Mitochondria (M) are identified by the presence of cristae (C). Immunogold beads (arrows) are identified in mitochondria and not in cytoplasm. Sections treated with normal rabbit serum in place of primary antibody did not show label.

modified proteins were higher in the nTg compared with that in the TgH mice in both the mitochondria and nucleus.

**Expression of *MnSOD* Reduced TPA-induced AP-1 Activation.** TPA has been demonstrated to cause an induction of AP-1 activity in the skin (8). Our results showed that AP-1 binding activity was activated as early as 6 h after TPA treatment in the nTg mice. In the TgH mice, the increase of AP-1 binding activity was delayed until 24 h after TPA treatment and was less prominent at almost all of the time points examined, with an exception at the 48-h time point (Fig. 2).

Table 1 Pathology results from mouse skin

TgH and nTg female mice received either DMSO alone or daily treatments with 4  $\mu$ g of TPA in DMSO, 5 days/week, for 14 weeks after a single application of 20 nm DMBA.

Strain	No. of mice	Tumor incidence	Papillomas/mouse	Total papillomas
nTg (DMBA + TPA)	9	78%	2.1	19
TgH (DMBA + TPA)	12	50%	0.75	9
nTg (DMSO)	2	0%	0	0
TgH (DMSO)	3	0%	0	0

Because the AP-1 complex may consist of homo- or heterodimers of various Fos, Jun, and Fra family members, supershift experiments were performed by preincubating samples used in the EMSA reaction with antibodies against members of the AP-1 family. Fig. 3 shows that an antibody against Jun D clearly shifted the AP-1 complex; less prominent shifted bands were seen with anti-c-Jun and anti-Jun B antibodies. There was no shift with antibodies to c-Fos and Fra-1. Western analysis (Fig. 4) further demonstrated that Jun D was the member of the Jun family that was increased in the skin within 24 h after TPA treatment. The presence of other Jun family members was undetectable in the same set of samples used for Jun D (data not shown). These results suggest that Jun D may play a major role in AP-1 activity, at least in the early stages of the TPA treatment.

**JNK Kinase Was Activated upon TPA Treatment.** JNK kinase was identified as a JNK and other jun family members kinase. To determine whether activation of AP-1 is associated with JNK activity, Western analysis of JNK kinase after TPA treatment was performed. Fig. 5 shows the results within 24 h. In the cytosolic fraction from the nTg mice, the levels of phosphorylated forms of JNK (pJNK) were slightly increased at 6 h after TPA treatment and significantly increased at 24 h after TPA treatment. In the TgH mice, the levels were increased at 24 h after TPA treatment. The increased level at 24 h in the nTg mice was higher than that in the TgH mice. These results suggested that JNK participated in tumor promotion by TPA, and overexpression of MnSOD may regulate the activation of pJNK, either by delaying or reducing its activation.

**PKC $\epsilon$  Was Activated upon TPA Treatment.** PKC is a family of serine/threonine protein kinases, which has been found to be involved in the mechanism of the action of TPA (10, 21). It is well established that TPA can directly activate PKC by binding to its regulatory domain, in turn leading to an increased expression of certain oncogenes (22).

We examined eight isoforms of PKC in skin tissue and found that six of them were expressed at a detectable level (PKC $\alpha$ , PKC $\beta$ I, PKC $\zeta$ , PKC $\beta$ II, PKC $\delta$ , and PKC $\epsilon$ ). Among these PKCs, the levels of PKC $\epsilon$  were increased in the nTg mice at 6 h after TPA treatment, but there was no increase in TgH mice (Fig. 6). The levels of other PKCs were not found to be significantly changed after TPA treatment (data not shown).

## DISCUSSION

It has been suggested that MnSOD, a primary antioxidant enzyme, may function as a new type of tumor suppressor gene for the following reasons: (a) many types of cultured tumor cells have reduced MnSOD activity when compared with their normal counterparts (1, 23, 24); (b) transformation of normal fibroblasts by SV40 virus leads to the reduction of MnSOD activity (4); (c) mutations in the *MnSOD* gene and its regulatory sequence have been observed in several types of human cancer (3, 25); and (d) overexpression of MnSOD reduces tumorigenicity and metastatic ability in a large number of experimental tumors *in vitro* and *in vivo* (5, 26, 27). However, the mechanisms by which MnSOD suppresses the malignant phenotype are unclear.

Cancer development is a multistage process that involves both the activation of proto-oncogenes and the inactivation of tumor suppressor genes (28). The mouse skin model of multistage carcinogenesis is an excellent model in which to study the biochemistry and molecular biology of cancer susceptibility. This is particularly true with regard to tumor promotion, a process that occurs in other organs and species including humans. The multistage model of carcinogenesis in mouse skin has, for >50 years, provided a conceptual framework from which to study the carcinogenesis process. However, most of the models developed focused on obtaining a large number of skin tumors/mouse, a condition rarely found in humans. In the present study, the incidence of skin tumors in B6C3F1 mice is high, but the number of papillomas/mouse is relatively low compared with other more sensitive mouse models (29, 30). Our finding, that overexpression of MnSOD in the skin in this model reduces the number and incidence of papillomas, provides direct evidence to support the involvement of superoxide-mediated mechanism(s) in the DMBA/TPA carcinogenesis process. Although free radicals and resulting oxidative stress have been shown to be involved in the carcinogenesis process, our results, which indicate that TPA rapidly increased the levels of 4-HNE-modified proteins in both mitochondria and nucleus and that increased expression of MnSOD in the mitochondria can reduce 4-HNE modified protein levels in both the mitochondria and the nucleus, provide important new evidence that TPA results in oxidative stress in both cellular compartments. These results confirm the link between the protection of mitochondria to reduction of oxidative injury in the nuclear compartment. This result is consistent with our previous studies in the embryonic fibroblast C3H10T1/2 cell line, which demonstrated a link between mitochondrial antioxidant status and radiation-induced neoplastic transformation (31).

Because tumor promotion is an important component of carcinogenesis in humans, the identification of genes that modify response(s) to tumor-promoting agents would be a significant advancement in our understanding of the genetic basis of susceptibility to cancer. The process of tumor promotion involves the production and maintenance of sustained cellular proliferation of epidermal cells (8). Changes induced by TPA are thought to result from epigenetic mechanisms, including activation of the cellular receptor protein kinase C. The initiation step of two-stage carcinogenesis has been described as the result of permanent genetic alterations in basal cells of the epidermis that make these cells resistant to signals for terminal differentiation (8). Mutational activation of the *Ha-ras* proto-oncogene is an early event clearly associated with chemical initiation of skin tumors (8). The process of skin tumor initiation appears to be similar in various mouse strains, and most data suggest that differences in response to tumor promoters are major determinants in controlling susceptibility to multistage skin carcinogenesis (32, 33).

In our mouse model, treatment with DMBA leads to *Ha-ras* mutation in both transgenic and nontransgenic mice (data not shown). However, after 14 weeks of TPA application, tumor incidence was

Table 2 Quantitative analysis of Immunogold labeling for 4-HNE-modified proteins in keratinocytes

The density of gold particles is mean  $\pm$  SD ( $\mu$ m<sup>2</sup>). Statistical analysis was performed by Student's *t* test.

	nTg control	nTg 6 h after TPA	TgH control	TgH 6 h after TPA
Cells counted	63	33	67	32
Cytoplasm	5.12 $\pm$ 2.28 <sup>a</sup>	6.98 $\pm$ 2.40 <sup>b</sup>	3.99 $\pm$ 2.00	6.98 $\pm$ 1.81 <sup>b</sup>
Nucleus	8.00 $\pm$ 5.52	27.37 $\pm$ 7.15 <sup>b,c</sup>	6.56 $\pm$ 2.67	14.30 $\pm$ 4.13 <sup>b</sup>
Mitochondria	9.12 $\pm$ 7.78	23.99 $\pm$ 14.00 <sup>b,c</sup>	6.63 $\pm$ 6.19	13.47 $\pm$ 11.60

<sup>a</sup> *P* < 0.01 compared with control TgH group.

<sup>b</sup> *P* < 0.01 compared with control group.

<sup>c</sup> *P* < 0.01 compared with TgH group.

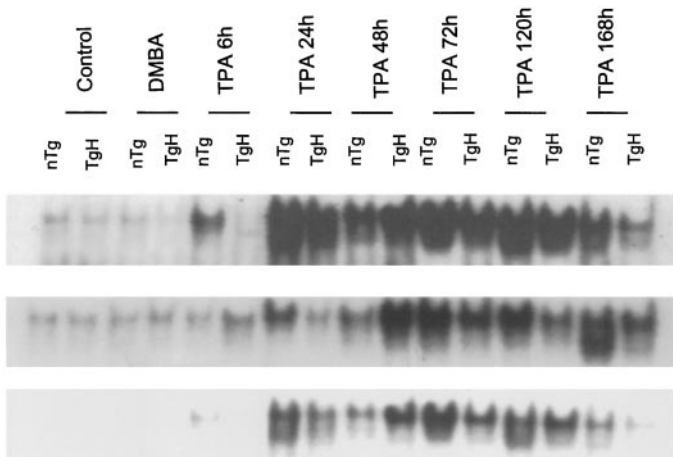


Fig. 2. EMSA detection of AP-1 binding activity in DMBA/TPA treated transgenic or nontransgenic mice (TPA was applied after DMBA treatment). Six  $\mu\text{g}$  of nuclear extract and radiolabeled AP-1 oligonucleotide were used. Three sets of samples from individual mouse skin are shown.

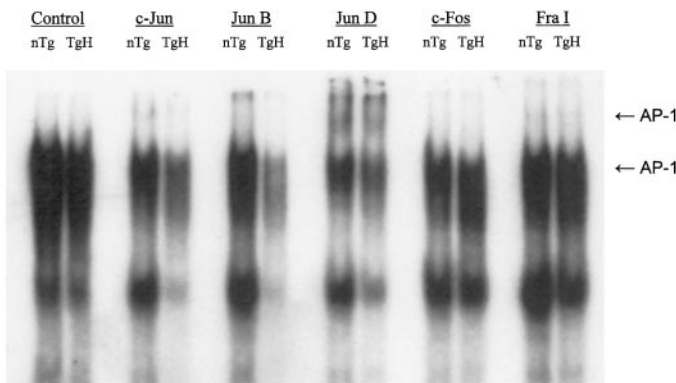


Fig. 3. Supershift identification of AP-1 family members that were involved in AP-1 induction by TPA (TPA was applied after DMBA treatment). The nuclear extract was preincubated with respective antibody to each AP-1 member, followed by the steps for EMSAs.

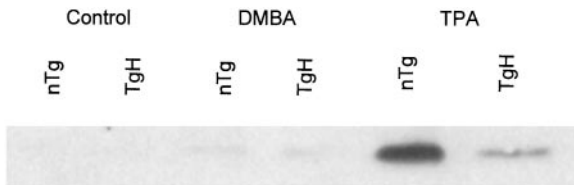


Fig. 4. Western analysis of the levels of Jun D protein in the nuclear extract from mouse skin. TPA was applied after DMBA treatment.

lower in TgH mice than nTg mice. The papillomas/mouse and total papillomas were also lower in the TgH mice. These data provide evidence that overexpression of MnSOD reduced tumorigenicity at the promotion step in this two-stage carcinogenesis model.

It is well recognized that DMBA or TPA treatment can induce oxidative stress (20, 34). We demonstrated for the first time that TPA application induced rapid oxidative stress at the subcellular level, as indicated by increased 4-HNE-modified protein levels in both the mitochondria and nucleus, and that overexpression of MnSOD reduced the levels of 4-HNE-modified proteins. Our model is consistent with the notion that oxidative stress participates in the carcinogenesis process. It has been shown *in vitro* that ROS can increase the activity of redox sensitive transcription factors including AP-1. Here we showed that the activation of AP-1 could be detected within 6 h after

TPA treatment in the nTg mice, which is consistent with the results that have been reported (8). In the TgH mice, the initial activation of AP-1 binding was delayed but reached a higher level than that in the nTg mice at 48 h. Because overexpression of MnSOD delayed and gradually reduced AP-1 activation, these results support the idea that inhibition of AP-1-mediated transcriptional activation is sufficient to suppress the tumorigenic phenotype of mouse epidermal cells. However, we could not rule out the possibility of TPA-induced activation of other transcription factors that were not investigated in this study. Our laboratory has established a MnSOD-transfected murine fibrosarcoma cell line, FSa-II cell, which exhibits low endogenous levels of MnSOD. We found that overexpression of MnSOD reduced the metastasis rate of fibrosarcoma cells transplanted into syngeneic mice (6). The reduction of tumor metastasis was consistent with our subsequent findings that overexpression of MnSOD in this cell line

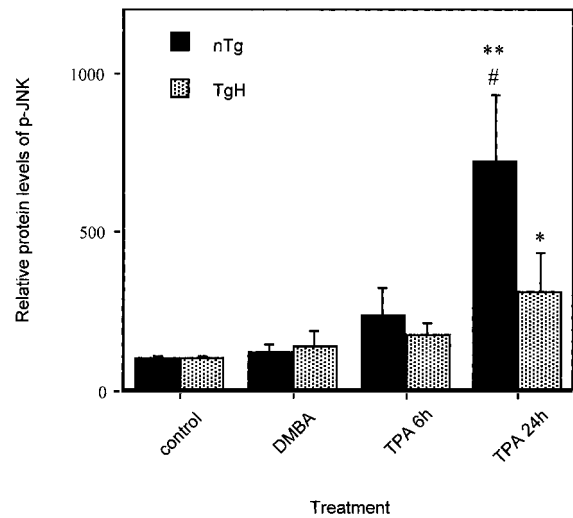


Fig. 5. The relative levels of pJNK in the cytosol fraction after DMBA/TPA treatment (TPA was applied after DMBA treatment). The relative densities of the pJNK protein bands were quantitated using Western blots from three sets of independent experiments. Statistical analysis was performed by using ANOVA. \*, difference from the vehicle control group,  $P < 0.05$ . \*\*, significant difference from the vehicle control group,  $P < 0.01$ ; #, difference from the TgH group,  $P < 0.05$ . Bars, SD.

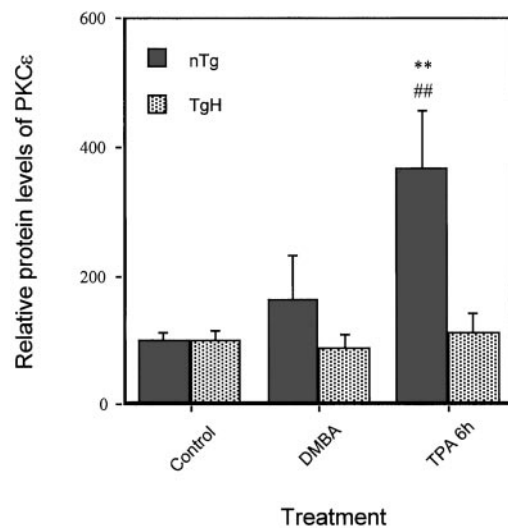


Fig. 6. The relative levels of PKC $\epsilon$  in the membrane fraction at 6 h after DMBA/TPA treatment (TPA was applied after DMBA treatment). The relative densities of the PKC $\epsilon$  protein bands were quantitated from Western blots. Data represent average result from four sets of independent experiments. Statistical analysis was performed using ANOVA. \*\*, significant difference from the vehicle control group,  $P < 0.01$ . ##, significant difference from the TgH group,  $P < 0.01$ . Bars, SD.

selectively reduced the binding activity of Jun-associated transcription factors (AP-1 and cyclic AMP-responsive element binding protein) but not NF $\kappa$ B or p53 (35). Taken together, the results from our previous work in established cancer cells and our current work in an *in vivo* model of carcinogenesis strongly implicates the modulation of AP-1-mediated pathways by MnSOD.

A number of posttranslational mechanisms are known to regulate AP-1 activity, including phosphorylation states of the Jun or Fos protein (36) and redox regulation of the Jun protein (37). The 4-HNE protein adduct data demonstrated that oxidative stress occurred rapidly in mice after TPA treatment. Thus, it is possible that changes in intracellular redox status may directly or indirectly modify the activation of AP-1. Our results from Western analysis, which indicates an increase in Jun protein and the presence of high levels of phosphorylated JNK at 24 h after TPA treatment in the nontransgenic mice, suggests the possibility of both transcriptional and posttranscriptional modulation. It has been suggested that increased amounts and posttranslational modifications of c-Jun, Fra-1, Fra-2, and ATF-2 proteins account for a high percentage of the increased AP-1 activity (38). c-Jun and ATF-2 proteins are phosphorylated by highly active JNK kinases present in tumor cells (38). It has been shown that JNK is involved in both cell growth and cell death pathways (39–42). For an example, Lee *et al.* (42) reported that expression of catalytically inactive, dominant-negative JNK1 protein is capable of suppressing persistent JNK activation as well as oxidative stress and cytotoxicity caused by glucose deprivation in MCF-7/ADR multidrug-resistant human breast adenocarcinoma cells. Our results suggested that JNK signaling mainly participates in growth-stimulatory responses. Furthermore, we found that members of the Jun but not Fos family are responsible for AP-1 binding activity. It is possible that our results are representative of an early stage of skin carcinogenesis.

Major insights into the mechanism of action of the phorbol esters and other tumor promoters were largely derived from the discovery of their interactions with PKC (10, 21, 43). The involvement of PKC, a TPA receptor, in the transcriptional regulation of TPA-inducible genes has been well established. In our mouse model, PKC $\epsilon$  was activated early after TPA treatment, and overexpression of MnSOD reduced PKC $\epsilon$  activation. We propose that in our mouse model, TPA treatment caused an activation of PKC $\epsilon$  leading to an activation of downstream JNK and AP-1 activities. The importance of PKC $\epsilon$  in DMBA/TPA skin carcinogenesis was demonstrated recently by the fact that overexpression of PKC $\epsilon$  in transgenic mice resulted in rapid formation of skin carcinomas (30, 44).

Overall, by using the MnSOD transgenic and nontransgenic littermates, we observed that tumor incidence and levels of oxidative stress were reduced, the levels/activities of AP-1 were suppressed or the induction was delayed, and the activation of PKC $\epsilon$  by TPA was also delayed in transgenic mice compared with their nontransgenic littermates, which is consistent with suppression of tumor formation. Thus, tumor suppression and antioxidant functions of MnSOD are indeed interrelated. These results not only provide direct links between reduction of oxidative stress induced by DMBA/TPA treatment to the development of papillomas but also identify a redox-sensitive signaling pathway leading to skin tumor promotion by TPA.

## ACKNOWLEDGMENTS

We thank Dr. Larry Oberley for antibodies against human MnSOD and Dr. Luke Szveda for antibodies against 4-HNE adducts. The technical assistance from Cathleen Hsu and Marcie Cole is appreciated.

## REFERENCES

- Oberley, L. W., and Buettner, G. R. Role of superoxide dismutase in cancer: a review. *Cancer Res.*, 39: 1141–1149, 1979.
- Sun, Y. Free radicals, antioxidant enzymes, and carcinogenesis. *Free Radicals Biol. Med.*, 8: 583–599, 1990.
- Xu, Y., Krishnan, A., Wan, X. S., Majima, H., Yeh, C. C., Ludewig, G., Kasarskis, E. J., and St. Clair, D. K. Mutations in the promoter reveal a cause for the reduced expression of the human manganese superoxide dismutase gene in cancer cells. *Oncogene*, 18: 93–102, 1999.
- Yan, T., Oberley, L. W., Zhong, W., and St. Clair, D. K. Manganese-containing superoxide dismutase overexpression causes phenotypic reversion in SV40-transformed human lung fibroblasts. *Cancer Res.*, 56: 2864–2871, 1996.
- Zhong, W., Oberley, L. W., Oberley, T. D., and St. Clair, D. K. Suppression of the malignant phenotype of human glioma cells by overexpression of manganese superoxide dismutase. *Oncogene*, 14: 481–490, 1997.
- Safford, S. E., Oberley, T. D., Urano, M., and St. Clair, D. K. Suppression of fibrosarcoma metastasis by elevated expression of manganese superoxide dismutase. *Cancer Res.*, 54: 4261–4265, 1994.
- Mukhtar, H., Mercurio, M. C., and Agarwal, R. Skin carcinogenesis: relevance to humans. In: H. Mukhtar (eds.), *Skin Cancer: Mechanisms and Human Relevance*, pp. 3–8. Boca Raton, FL: CRC Press, 1995.
- Bowden, G. T., Finch, J., Domann, F., and Krieg, P. Molecular mechanisms involved in skin tumor initiation, promotion and progression. In: H. Mukhtar (eds.), *Skin Cancer: Mechanisms and Human Relevance*, pp. 99–111. Boca Raton, FL: CRC Press, 1995.
- Iversen, O. H. Of mice and men: a critical reappraisal of the two-stage theory of carcinogenesis. *Crit. Rev. Oncog.*, 6: 357–405, 1995.
- Nishizuka, Y. The role of protein kinase C in cell surface signal transduction and tumor promotion. *Nature (Lond.)*, 308: 693–698, 1984.
- Troll, W. Prevention of cancer by agents that suppress oxygen radical formation. *Free Radicals Res. Commun.*, 12–13 (Part 2): 751–757, 1991.
- Slaga, T. J. Inhibition of the induction of cancer by antioxidants. *Adv. Exp. Med. Biol.*, 369: 1671–1674, 1995.
- McCord, J. M., The evolution of free radicals and oxidative stress. *Am. J. Med.*, 108: 652–659, 2000.
- Yen, H. C., Oberley, T. D., Vichitbandha, S., Ho, Y. S., and St. Clair, D. K. The protective role of manganese superoxide dismutase against Adriamycin-induced acute cardiac toxicity in transgenic mice. *J. Clin. Investig.*, 98: 1253–1260, 1996.
- Chirgwin, J. M., Przybyla, A. E., MacDonald, R. J., and Rutter, W. J. Isolation of biologically active ribonucleic acid from sources enriched in ribonuclease. *Biochemistry*, 18: 5294–5299, 1979.
- St. Clair, D. K., and Holland, J. C. Complementary DNA encoding human colon cancer manganese superoxide dismutase and the expression of its gene in human cells. *Cancer Res.*, 51: 939–943, 1991.
- Ria, F., Landriscina, M., and Galeotti, T. Preparation of a monoclonal antibody against rat MnSOD, using a COOH-terminal peptide. *Biochem. Biophys. Res. Commun.*, 195: 697–703, 1993.
- Das, K. C., Guo, X. L., and White, C. W. Protein kinase C $\delta$ -dependent induction of manganese superoxide dismutase gene expression by microtubule-active anticancer drugs. *J. Biol. Chem.*, 273: 34639–34645, 1998.
- Nakamura, Y., Kawamoto, N., Ohto, Y., Torikai, K., Murakami, A., and Ohigashi, H. A diacytlenic spiroketal enol ether epoxide, AL-1, from *Artemisia lactiflora* inhibits 12-*O*-tetradecanoylphorbol-13-acetate-induced tumor promotion possibly by suppression of oxidative stress. *Cancer Lett.*, 140: 37–45, 1999.
- Isbir, T., Yaylim, I., Aydin, M., Ozturk, O., Koyuncu, H., Zeybek, U., Agachan, B., and Yilmaz, H. The effects of *Brassica oleraceae* var capitata on epidermal glutathione and lipid peroxides in DMBA-initiated TPA-promoted mice. *Anticancer Res.*, 20: 219–224, 2000.
- Blumberg, P. M. *In vitro* studies on the mode of action of the phorbol esters, potent tumor promoters. *Crit. Rev. Toxicol.*, 8: 153–197, 1980.
- Castagna, M., Takai, Y., Kaibuchi, K., Sano, K., Kikkawa, U., and Nishizuka, Y. Direct activation of calcium-activated, phospholipid-dependent protein kinase by tumor-promoting phorbol esters. *J. Biol. Chem.*, 257: 7847–7851, 1982.
- St. Clair, D. K., and Oberley, L. W. Manganese superoxide dismutase expression in human cancer cells: a possible role of mRNA processing. *Free Radicals Res. Commun.*, 2: 771–778, 1991.
- Sun, Y., Oberley, L. W., Oberley, T. D., Elwell, J. H., and Sierra-Rivera, E. Lowered antioxidant enzymes in spontaneously transformed embryonic mouse liver cells in culture. *Carcinogenesis (Lond.)*, 14: 1457–1463, 1993.
- Zhang, H. J., Yan, T., Oberley, T. D., and Oberley, L. W. Comparison of effects of two polymorphic variants of manganese superoxide dismutase on human breast MCF-7 cancer cell phenotype. *Cancer Res.*, 59: 6276–6283, 1999.
- Church, S. L., Grant, J. W., Ridnour, L. A., Oberley, L. W., Swanson, P. E., Meltzer, P. S., and Trent, J. M. Increased manganese superoxide dismutase expression suppresses the malignant phenotype of human melanoma cells. *Proc. Natl. Acad. Sci. USA*, 90: 3113–3117, 1993.
- Urano, M., Kuroda, M., Reynolds, R., Oberley, T. D., and St. Clair, D. K. Expression of manganese superoxide dismutase reduces tumor control radiation dose: gene-radiotherapy. *Cancer Res.*, 55: 2490–2493, 1995.
- Angel, J. M., and DiGiovanni, J. Genetics of skin tumor promotion. *Prog. Exp. Tumor Res.*, 35: 143–157, 1999.
- Reddig, P. J., Dreckschmidt, N. E., Ahrens, H., Simsiman, R., Tseng, C. P., Zou, J., Oberley, T. D., and Verma, A. K. Transgenic mice overexpressing protein kinase C $\delta$  in the epidermis are resistant to skin tumor promotion by 12-*O*-tetradecanoylphorbol-13-acetate. *Cancer Res.*, 59: 5710–5718, 1999.

30. Reddig, P. J., Dreckschmidt, N. E., Zou, J., Bourguignon, S. E., Oberley, T. D., and Verma, A. K. Transgenic mice overexpressing protein kinase C epsilon in their epidermis exhibit reduced papilloma burden but enhanced carcinoma formation after tumor promotion. *Cancer Res.*, *60*: 595–602, 2000.
31. St. Clair, D. K., Wan, X. S., Oberley, T. D., Muse, K. E., and St. Clair, W. H. Suppression of radiation-induced neoplastic transformation by overexpression of mitochondrial superoxide dismutase. *Mol. Carcinog.*, *6*: 238–242, 1992.
32. Chouroulinkov, I., Lasne, C., Phillips, D., and Grover, P. Sensitivity of the skin of different mouse strains to the promoting effect of 12-*O*-tetradecanoyl-phorbol-13-acetate. *Bull. Cancer (Paris)*, *75*: 557–565, 1988.
33. Naito, M., and DiGiovanni, J. Genetic background and development of skin tumors. *Carcinog. Compr. Surv.*, *11*: 187–212, 1989.
34. Khajuria, A., Thusu, N., Zutshi, U., and Bedi, K. L. Piperine modulation of carcinogen induced oxidative stress in intestinal mucosa. *Mol. Cell. Biochem.*, *189*: 113–118, 1998.
35. Kinningham, K. K., and St. Clair, D. K. Overexpression of manganese superoxide dismutase selectively modulates the activity of Jun-associated transcription factors in fibrosarcoma cells. *Cancer Res.*, *57*: 5265–5271, 1997.
36. Boyle, W. J., Smeal, T., Defize, L. H., Angel, P., Woodgett, J. R., Karin, M., and Hunter, T. Activation of protein kinase C decreases phosphorylation of c-Jun at sites that negatively regulate its DNA-binding activity. *Cell*, *64*: 573–584, 1991.
37. Xanthoudakis, S., Miao, G., Wang, F., Pan, Y-C. E., and Curran, T. Redox activation of fos-jun DNA binding activity is mediated by a DNA repair enzyme. *EMBO J.*, *11*: 3323–3335, 1992.
38. Zoumpourlis, V., Papassava, P., Linardopoulos, S., Gillespie, D., Balmain, A., and Pintzas, A. High levels of phosphorylated c-Jun, Fra-1, Fra-2 and ATF-2 proteins correlate with malignant phenotypes in the multistage mouse skin carcinogenesis model. *Oncogene*, *19*: 4011–4021, 2000.
39. Xia, Z., Dickens, M., Raingeaud, J., Davis, R. J., and Greenberg, M. E. Opposing effects of ERK and JNK-p38 MAP kinases on apoptosis. *Science (Wash. DC)*, *270*: 1326–1331, 1995.
40. Smith, A., Ramos-Morales, F., Ashworth, A., and Collins, M. A role for JNK/SAPK in proliferation, but not apoptosis. *Curr. Biol.*, *7*: 893–896, 1997.
41. Bost, F., McKay, R., Dean, N., and Mercola, D. The JUN kinase/stress-activated protein kinase pathway is required for epidermal growth factor stimulation of growth of A549 lung carcinoma cells. *J. Biol. Chem.*, *272*: 33422–33429, 1997.
42. Lee, Y. J., Galoforo, S. S., Sim, J. E., Ridnour, L. A., Choi, J., Forman, H. J., Corry, P. M., Spitz, D. R. Dominant-negative Jun N-terminal protein kinase (JNK-1) inhibits metabolic oxidative stress during glucose deprivation in a human breast carcinoma cell line. *Free Radical Biol. Med.*, *28*: 575–584, 2000.
43. Tseng, C. P., Kim, Y. J., Kumar, R., and Verma, A. K. Involvement of protein kinase C in the transcriptional regulation of 12-*O*-tetradecanoylphorbol-13-acetate-inducible genes modulated by AP-1 or non-AP-1 transacting factors. *Carcinogenesis (Lond.)*, *15*: 707–711, 1994.
44. Jansen, A. P., Verwiebe, E. G., Dreckschmidt, N. E., Wheeler, D. L., Oberley, T. D., and Verma, A. K. Protein kinase Cε transgenic mice: a unique model for metastatic squamous cell carcinoma. *Cancer Res.*, *61*: 808–812, 2001.